Questioning numerical integration methods for microsphere (and microplane) constitutive equations

Erwan Verron

Questioning numerical integration methods for microsphere (and microplane) constitutive equations

Erwan Verron

École Centrale de Nantes, Institut de Recherche en Génie Civil et Mécanique (GeM) – UMR CNRS 6183, BP 92101, 44321 Nantes cedex 3, France

In the last few years, more and more complex microsphere models have been proposed to predict the mechanical response of various polymers. Similarly than for microplane mod els, they consist in deriving a one dimensional force vs. stretch equation and to integrate it over the unit sphere to obtain a three dimensional constitutive equation. In this context, the focus of authors is laid on the physics of the one dimensional relationship, but in most of the case the influence of the integration method on the prediction is not investigated.

Here we compare three numerical integration schemes: a classical Gaussian scheme, a method based on a regular geometric meshing of the sphere, and an approach based on spherical harmonics. Depending on the method, the number of integration points may vary from 4 to 983,040! Considering simple quantities, i.e. principal (large) strain invariants, it is shown that the integration method must be carefully chosen. Depending on the quantities retained to described the one dimensional equation and the required error, the perfor mances of the three methods are discussed. Consequences on stress strain prediction are illustrated with a directional version of the classical Mooney Rivlin hyperelastic model. Finally, the paper closes with some advices for the development of new microsphere con stitutive equations.

1. Introduction

In the last few years, number of authors have proposed constitutive equations inspired by the microsphere model of Miehe et al. (2004) for various large strain non linear materials, e.g. anisotropy of the Mullins effect in elas tomers (Diani et al., 2006; Dargazany and Itskov, 2009), behaviour of blood vessels (Alastrué et al., 2009), ageing and fracture of rubber (Dal and Kaliske, 2009), non woven fabrics (Tkachuk and Linder, 2012), thermosets (Fleischhauer et al., 2012), strain induced crystallization in rubber (Mistry and Govindjee, 2014), stress softening in rubber and soft tissues (Rebouah and Chagnon, 2014,), electro active polymers (Zäh and Miehe, 2015),...This approach is in line with the chain models for rubber like materials: 3 chain (James and Guth, 1943), 4 chain (Flory and Rehner, 1943), 8 chain (Arruda and Boyce, 1993) and full network (Treloar and Riding, 1979; Wu and van der Giessen, 1993) models. Roughly speaking the development of such constitutive equations consists in (i) deriving the force vs. stretch equation for a polymer chain, (ii) relating the chain stretch to the macroscopic stretch ratio in a given direction, and finally (iii) integrating the force vs. stretch equation over the unit sphere to calculate the stress tensor. In most of the cases, authors focus their attention on steps (i) and (ii), invoking more or less complex concepts of poly mer physics. In the past, step (iii) for chain models was performed analytically. Nevertheless, the complexity of microsphere constitutive equations necessitates the use of numerical integration (also referred to as cubature (Hesse et al., 2010)) methods over the unit sphere. Such methods consist in discretizing the unit sphere, denoted

E-mail address: erwan.verron@ec-nantes.fr

$\mathcal{S}$, with a set of n points $(\mathbf{u}_j)_{j\ 1,\dots,n} \in \mathcal{S}$ and in transforming the integral of a function of directions $F(\mathbf{u})$ (scalar, vecto rial or tensorial) into a weighted sum:

$$\frac{1}{|\mathcal{S}|}\iint_{\mathcal{S}} F(\mathbf{u})\, d^2\Omega \approx \sum_{j\ 1}^{n} w_j F(\mathbf{u}_j), \tag{1}$$

where $|\mathcal{S}|$ is the surface of the sphere, $d^2\Omega$ the solid angle and $(w_j)_{j\ 1,\dots,n}$ the weights. Choosing an integration method reduces to the definition of n, $(w_j)_{j\ 1,\dots,n}$ and $(\mathbf{u}_j)_{j\ 1,\dots,n}$. In the large majority of the studies, authors retain the method proposed by Bažant and Oh (1986) and especially the fully symmetric formulation with n 42, i.e. n 21 over the hemisphere.

It is to note here that the method of Bažant and Oh (1986) has been developed for the computation of consti tutive equations for concrete and rock in the 80s and extended later to brittle plastic materials. These constitu tive equations are referred to as *microplane models* and, similarly to the above mentioned microsphere models, consists in deriving a one dimensional stress strain relationship and to integrate it over the unit sphere. By contrast to microsphere models, small strain were first considered (large strain were investigated later) and these models involve more complex dissipative mechanisms such as plasticity and damage. As the present paper focuses on large strain, and also because the author is not a specialist in the field, only emblematic papers are mentioned (Bažant and Gambarova, 1984; Bažant and Oh, 1985; Bažant and Prat, 1988; Carol and Bažant, 1997; Bažant et al., 2000). For more precise and relevant informa tions, the reader can refer to the short historical review proposed in Brocca and Bažant (2000) and to the most recent papers on the subject.

Even if the 42 points version of the Bažant and Oh method is widely applied, some authors have analysed its performance. Two major limitations have been investi gated. First, its ability to reflect the isotropy or anisotropy of the considered constitutive equation depends on the distribution of integration points over the sphere, and can be for example estimated by the smallest difference between minimum and maximum values of the integral obtained for all rigid body rotations of the set of integration points as emphasized by Bažant and Oh (1986) themselves (Ehret et al., 2010). Second, its ability to integrate non smooth functions questions Gaussian schemes that consist in representing functions by polyno mials (Badel and Leblond, 2004). These aforementioned difficulties have been investigated by several authors for both microsphere (Alastrué et al., 2009; Ehret et al., 2010; Gillibert et al., 2010) and microplane (Qiu and Crouch, 1997; Badel and Leblond, 2004; Cheng and Shen, 2010; Levasseur et al., 2013) models.

The present paper aims to demonstrate that the cubature method has to be considered as a part of the constitutive equation because the appropriate method can be chosen in regards to the mechanical quantities involved in the model. More precisely, our study is devoted to microsphere models, i.e. the framework of finite strain is considered; nevertheless, we believe that the results may also apply to microplane models. In order to investigate the quality of cubature schemes, three integration methods are considered: the classical Gaussian scheme of Bažant and Oh (1986), the geometrical meshing approach of Badel and Leblond (2004) and the extremal points method based on spherical harmonics of Sloan and Womersley (2004). In our opinion, these three methods are representa tive of possible choices for cubature over the sphere. For these methods, various numbers of integration points are considered.

The methods are evaluated and compared through their ability to calculate the principal strain invariants in large strain. In fact, principal strain invariants are representative of the mechanical quantities involved in the force vs. stretch relationship which are integrated in microsphere models, e.g. the first invariant is related to chain stretch and the second one is related to the change in tube diameter for tube models (Kearsley, 1989). It will be shown in the paper that the study of these simple examples is sufficient to question integration methods. Moreover, to illustrate the possible consequences on stress strain predictions, a directional version of the Mooney Rivlin model is investigated. In Section 2 the expression of the strain invariants in terms of integrals are derived following the proposal of Carol et al. (2004); and the three cubature methods are briefly presented in Section 3. Section 4 pre sents the results and the discussion: first, errors induced by the methods are analysed; then the choice of relevant method and number of integration points, depending on the prescribed error and mechanical quantities that must be integrated, is addressed; finally consequences on stress strain prediction are highlighted. Finally, Section 5 closes the paper with some proposals about the choice of the integration method in the derivation of constitutive equations.

2. Closed-form expressions of integrals over the unit sphere

In this section, the closed form formulae for integrals of some strain quantities over the unit sphere are derived. For this purpose, the results established by Carol et al. (2004) are revisited.[1] It is to note that other authors have proposed formulae to express invariants quantities in integral form, among them we can mention Kearsley (1989), Beatty (2003), Puso (2003), and Ehret et al. (2010).

2.1. Deformation

Consider a material point in a given body, where the deformation gradient is denoted $\mathbf{F}$. The corresponding right and left Green Lagrange strain tensors are respectively

$$\mathbf{C} \quad \mathbf{F}^T\mathbf{F} \quad \text{and} \quad \mathbf{B} \quad \mathbf{F}\mathbf{F}^T \tag{2}$$

and their common principal invariants are

[1] The author highly recommend this paper and especially its remarkable Appendices B and C to the reader.

$$I_1 \quad \mathrm{tr}\cdot, \tag{3}$$

$$I_2 \quad \frac{1}{2}\Big[(\mathrm{tr}\cdot)^2 \quad \mathrm{tr}(\cdot^2)\Big], \tag{4}$$

$$I_3 \quad \det\cdot, \tag{5}$$

where stands for **C** and **B**.

Consider the unit sphere $\mathcal{S}$ of surface $|\mathcal{S}|$ (4π) at the material point and its deformed configuration, as sketched in 2D in Fig. 1(a) and (b), respectively. For a material direction **u**, the stretch in this direction (called the *microplane stretch* in Carol et al. (2004)) is

$$\lambda\mathbf{n} \quad \mathbf{F}\mathbf{u}, \tag{6}$$

where λ $\|\mathbf{F}\mathbf{u}\|$ and **n** is a unit vector; the change in oriented surface $dA\mathbf{u}$ is given by the Nanson formula

$$da\mathbf{n} \quad JdA\mathbf{F}^{T}\mathbf{u}, \tag{7}$$

where $\bar{\mathbf{n}}$ is a unit vector, J is the Jacobian of the deformation ($\det\mathbf{F}$ $\sqrt{I_3}$) and the superscript ^{T} stands for the transpose of the inverse.

Next, we consider the deformation gradient $\mathbf{F}^{T}$ that transforms the unit sphere into an ellipse (an ellipsoid in 3D) orthogonal to the conventional deformed configuration considered above. As shown in Fig. 1(c), we define the stretch $\bar{\lambda}$ (called the *microplane thickening* in Carol et al. (2004)) such that

$$\lambda^{-1}\mathbf{n} \quad \mathbf{F}^{T}\mathbf{u} \tag{8}$$

and the change in the oriented surface $dA\mathbf{u}$

$$da\mathbf{n} \quad J^{-1}dA\mathbf{F}\mathbf{u}. \tag{9}$$

Note that the latter expression is derived by replacing **F** by $\mathbf{F}^{T}$ in Eq. (7).

2.2. Integration over the unit sphere $\mathcal{S}$

Denoting $d^2\Omega$ the solid angle ($\sin\theta d\phi d\theta$ with the classical spherical coordinates) which contains unit direction vectors **u**, for a given function $F(\mathbf{u})$ which can be scalar, vectorial or tensorial, we define the following averaging integral operator

$$\langle F(\mathbf{u})\rangle \quad \frac{1}{|\mathcal{S}|}\iint_{\mathcal{S}} F(\mathbf{u})\,d^2\Omega. \tag{10}$$

As examples,

$$\frac{1}{|\mathcal{S}|}\iint_{\mathcal{S}} d^2\Omega \quad 1 \tag{11}$$

and

$$\langle\mathbf{u}\otimes\mathbf{u}\rangle \quad \frac{1}{|\mathcal{S}|}\iint_{\mathcal{S}}\mathbf{u}\otimes\mathbf{u}\,d^2\Omega \quad \frac{1}{3}\mathbf{I}, \tag{12}$$

where **I** is the 3×3 identity tensor.

Next, in order to extend the previous averaging operator Eq. (10) to functions of **n** and $\bar{\mathbf{n}}$, the corresponding solid angles have to be determined. Their derivation has been proposed in the Appendix B of Carol et al. (2004) and are recalled here. As shown in Fig. 2(a) and (b), as vectors **u** fill the solid angle $d^2\Omega$, vectors **n** fill the solid angle $d^2\omega$ defined by the infinitesimal surface ds obtained by the projection of $da\bar{\mathbf{n}}$ over **n** divided by the square of the radius of the sphere that intersects the ellipsoid at the given point, i.e. λ^2:

$$d^2\omega \quad \frac{ds}{\lambda^2} \quad \frac{(da\mathbf{n})\cdot\mathbf{n}}{\lambda^2}, \tag{13}$$

that leads to

$$d^2\omega \quad \frac{JdA\mathbf{F}^{-T}\mathbf{u}\cdot\mathbf{F}\mathbf{u}/\lambda}{\lambda^2} \quad \frac{JdA}{\lambda^3} \quad J\lambda^{-3}d^2\Omega. \tag{14}$$

Similarly, considering the deformation gradient $\mathbf{F}^{-T}$ and following a similar derivation, the solid angle defined in Fig. 2(c) is

$$d^2\omega \quad \frac{ds}{(\lambda^{-1})^2} \quad \frac{da\mathbf{n}\cdot\mathbf{n}}{(\lambda^{-1})^2}, \tag{15}$$

that leads to

$$d^2\omega \quad \frac{dA\mathbf{F}\mathbf{u}}{J\lambda^{-2}}\cdot\frac{\mathbf{F}^{-T}\mathbf{u}}{\lambda^{-1}} \quad J^{-1}\lambda^3 dA \quad J^{-1}\lambda^3 d^2\Omega. \tag{16}$$

Finally, considering that the unit spheres are identical in the three states ($\mathcal{S}$ $\mathcal{S}'$ $\mathcal{S}''$ in Fig. 2(a) (c)), the counterparts of Eq. (11) are

$$\frac{1}{|\mathcal{S}|}\iint_{\mathcal{S}} d^2\omega \quad \frac{1}{|\mathcal{S}|}\iint_{\mathcal{S}} d^2\omega \quad 1. \tag{17}$$

Using the relationships Eqs. (14) and (16), Eq. (12) transforms into

$$\frac{1}{|\mathcal{S}|}\iint_{\mathcal{S}}\mathbf{n}\otimes\mathbf{n}\,d^2\omega \quad \frac{1}{|\mathcal{S}|}\iint_{\mathcal{S}}\mathbf{n}\otimes\mathbf{n}J\lambda^{-3}d^2\Omega \quad J\langle\lambda^{-3}\mathbf{n}\otimes\mathbf{n}\rangle \quad \frac{1}{3}\mathbf{I} \tag{18}$$

and

$$\frac{1}{|\mathcal{S}|}\iint_{\mathcal{S}}\mathbf{n}\otimes\mathbf{n}\,d^2\omega \quad \frac{1}{|\mathcal{S}|}\iint_{\mathcal{S}}\mathbf{n}\otimes\mathbf{n}J^{-1}\lambda^3 d^2\Omega \quad J^{-1}\langle\lambda^3\mathbf{n}\otimes\mathbf{n}\rangle \quad \frac{1}{3}\mathbf{I}. \tag{19}$$

2.3. Integral formula for strain tensors and invariants

2.3.1. Strain tensors

The integral expressions of the left Cauchy Green strain tensor **B** are obtained by applying two pushforward operations, as clearly defined in Gurtin et al. (2010, pp. 95 97) and denoted $\mathbb{P}^{-1}$ and $\underline{\mathbb{P}}^{-1}$, to the material expression of the identity tensor Eq. (12). First, left and right multiplying Eq. $(12)_2$ respectively by **F** and $\mathbf{F}^T$, and invoking the definition of λ (Eq. (6)) leads to

$$\frac{1}{3}\underline{\mathbb{P}}^{-1}[\mathbf{I}] \quad \frac{1}{3}\mathbf{F}\mathbf{I}\mathbf{F}^{T} \quad \frac{1}{3}\mathbf{B} \quad \frac{1}{|\mathcal{S}|}\iint_{\mathcal{S}}(\mathbf{F}\mathbf{u})\otimes(\mathbf{F}\mathbf{u})\,d^2\Omega \quad \frac{1}{|\mathcal{S}|}\iint_{\mathcal{S}}\lambda^2\mathbf{n}\otimes\mathbf{n}\,d^2\Omega \tag{20}$$

and finally:

$$\mathbf{B} \quad 3\langle\lambda^2\mathbf{n}\otimes\mathbf{n}\rangle. \tag{21}$$

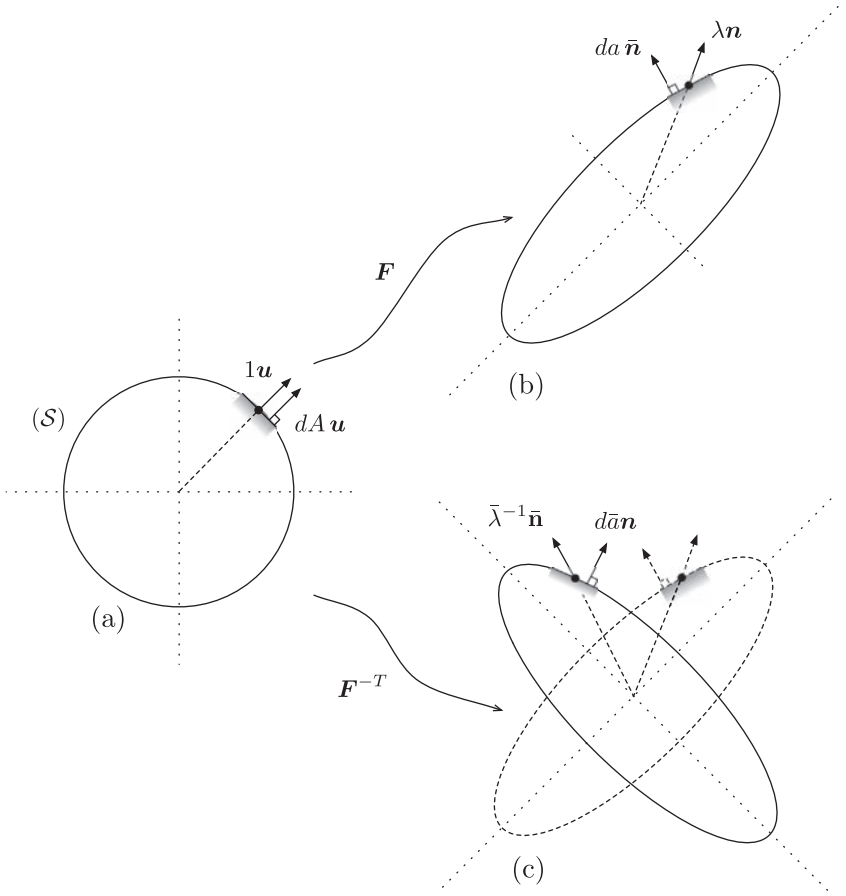

Fig. 1. Deformation of the unit sphere.

Similarly, left and right multiplying Eq. $(12)_2$ respectively by $\mathbf{F}^{T}$ and $\mathbf{F}^{1}$, and invoking the definition of $\bar{\lambda}$ (Eq. (8)) leads to

$$\frac{1}{3}\mathbb{P}^{1}[\mathbf{I}] \quad \frac{1}{3}\mathbf{F}^{T}\mathbf{I}\mathbf{F}^{1} \quad \frac{1}{3}(\mathbf{F}\mathbf{F}^{T})^{1} \quad \frac{1}{3}\mathbf{B}^{1} \quad \frac{1}{|\mathcal{S}|}\iint_{\mathcal{S}}(\mathbf{F}^{T}\mathbf{u})\otimes(\mathbf{F}^{T}\mathbf{u})\,d^2\Omega \quad \frac{1}{|\mathcal{S}|}\iint_{\mathcal{S}}\lambda^{2}\mathbf{n}\otimes\mathbf{n}\,d^2\Omega \tag{22}$$

and finally to

$$\mathbf{B}^{1} \quad 3\langle\lambda^{2}\mathbf{n}\otimes\mathbf{n}\rangle. \tag{23}$$

In the same manner, the integral expressions of the right Cauchy Green strain tensor $\mathbf{C}$ are derived by two pullback operations, also described in Gurtin et al. (2010, pp. 95 97) and denoted $\mathbb{P}$ and $\underline{\mathbb{P}}$, applied to the spatial expressions of the identity tensor Eqs. (18) and (19). First, note that Eq. (8) can be written as

$$\mathbf{F}^{T}\mathbf{n} \quad \lambda\mathbf{u}. \tag{24}$$

Then, using Eq. $(19)_2$, we have

$$\frac{1}{3}\mathbb{P}[\mathbf{I}] \quad \frac{1}{3}\mathbf{F}^{T}\mathbf{I}\mathbf{F} \quad \frac{1}{3}\mathbf{C} \quad \frac{1}{|\mathcal{S}|}\iint_{\mathcal{S}}(\mathbf{F}^{T}\mathbf{n})\otimes(\mathbf{F}^{T}\mathbf{n})J^{1}\lambda^{3}d^2\Omega \quad J^{1}\frac{1}{|\mathcal{S}|}\iint_{\mathcal{S}}\lambda^{5}\mathbf{n}\otimes\mathbf{n}\,d^2\Omega \tag{25}$$

and finally

$$\mathbf{C} \quad 3J^{1}\langle\lambda^{5}\mathbf{n}\otimes\mathbf{n}\rangle. \tag{26}$$

Considering now the expression of the identity tensor given by Eq. $(18)_2$ and

$$\mathbf{F}^{1}\mathbf{n} \quad \lambda^{1}\mathbf{u}, \tag{27}$$

we have

$$\frac{1}{3}\underline{\mathbb{P}}[\mathbf{I}] \quad \frac{1}{3}\mathbf{F}^{1}\mathbf{I}\mathbf{F}^{T} \quad \frac{1}{3}\mathbf{C}^{1} \quad \frac{1}{|\mathcal{S}|}\iint_{\mathcal{S}}(\mathbf{F}^{1}\mathbf{n})\otimes(\mathbf{F}^{1}\mathbf{n})J\lambda^{3}d^2\Omega \quad J\frac{1}{|\mathcal{S}|}\iint_{\mathcal{S}}\lambda^{5}\mathbf{n}\otimes\mathbf{n}\,d^2\Omega \tag{28}$$

and finally

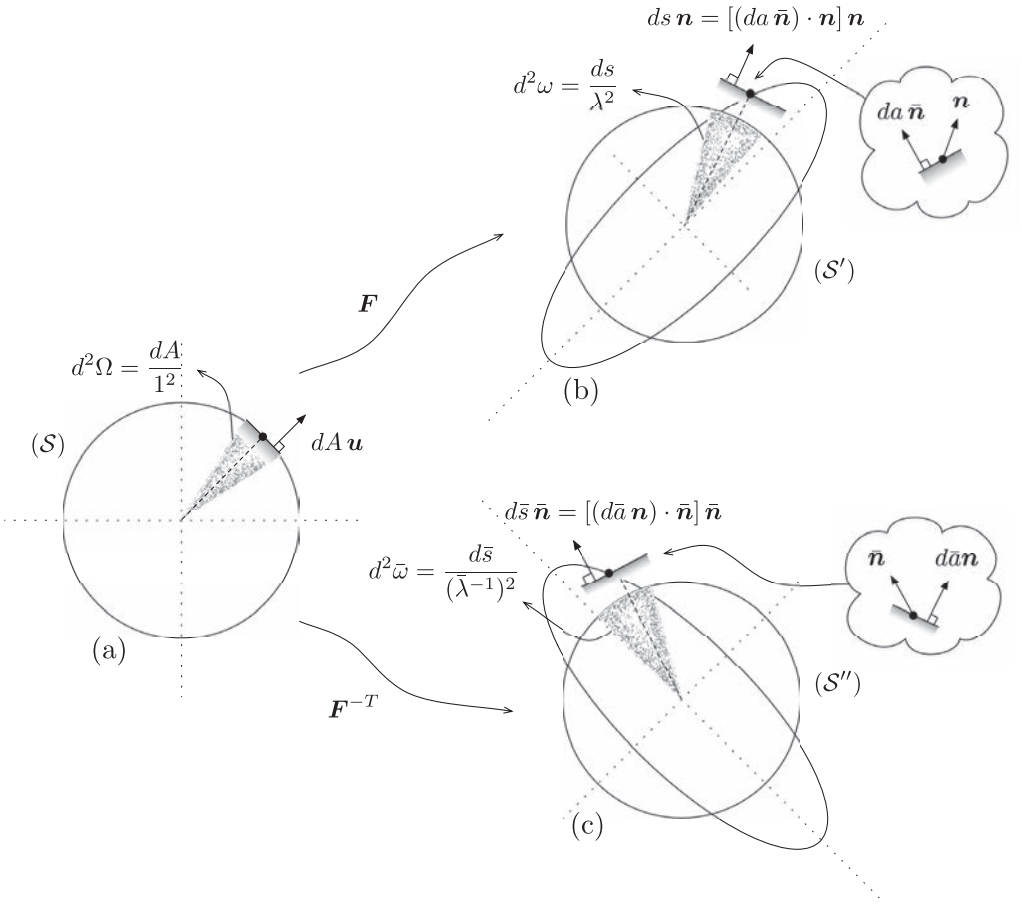

Fig. 2. Solid angles.

$$\mathbf{C}^{-1} \quad 3J\langle\lambda^{-5}\mathbf{n}\otimes\mathbf{n}\rangle. \tag{29}$$

2.3.2. Principal strain invariants

As stated by Eq. (3), the first invariant I_1 is the trace of both **C** and **B**. Noting that $\mathbf{I} : (\mathbf{a}\otimes\mathbf{a}) \quad 1$ for all unit vector **a**, Eq. (26) leads to

$$I_1 \quad \mathrm{tr}\mathbf{C} \quad \mathbf{I} : \mathbf{C} \quad 3J^{-1}\langle\lambda^5\rangle. \tag{30}$$

Similarly, Eq. (21) gives

$$I_1 \quad \mathrm{tr}\mathbf{B} \quad \mathbf{I} : \mathbf{B} \quad 3\langle\lambda^2\rangle. \tag{31}$$

In order to derive formula for I_2, we first invoke the Cayley Hamilton theorem which states that a given tensor **A** satisfies its own characteristic polynomial

$$\mathbf{A}^3 \quad I_1(\mathbf{A})\mathbf{A}^2 + I_2(\mathbf{A})\mathbf{A} \quad I_3(\mathbf{A})\mathbf{I} \quad 0. \tag{32}$$

If **A** is invertible, multiplying this equation by $\mathbf{A}^{-1}$ gives

$$\mathbf{A}^{-1} \quad I_3(\mathbf{A})^{-1}\left[\mathbf{A}^2 \quad I_1(\mathbf{A})\mathbf{A} + I_2(A)\mathbf{I}\right] \tag{33}$$

and double contraction with **I** leads to

$$\mathrm{tr}\mathbf{A}^{-1} \quad I_3(\mathbf{A})^{-1}\left[\mathrm{tr}\mathbf{A}^2 \quad I_1(\mathbf{A})^2 + 3I_2(A)\right] \quad J^{-2}I_2(\mathbf{A}). \tag{34}$$

Applying this equation to both **C** (Eq. (29)) and **B** (Eq. (23)) gives

$$I_2 \quad 3J^3\langle\lambda^{-5}\rangle \quad 3J^2\langle\lambda^{-2}\rangle. \tag{35}$$

Finally, contracting Eqs. $(18)_3$ and $(19)_3$ with **I** permits to obtain the two following expressions for I_3:

$$I_3 \quad J^2 \quad \langle\lambda^{-3}\rangle^{-2} \quad \langle\lambda^3\rangle^2. \tag{36}$$

Table 1 sums up the previous results.

3. Three methods of numerical integration on the unit sphere

As mentioned in the Introduction, numerical integration over the sphere consists in approximating the previous averaging operator Eq. (10) (Hesse et al., 2010):

$$\langle f\rangle \quad \frac{1}{|\mathcal{S}|}\iint_{\mathcal{S}} F(\mathbf{u})\,d^2\Omega \approx \sum_{j\ 1}^{n} w_j F(\mathbf{u}_j)$$

for a given scalar, vectorial or tensorial function F ($(w_j)_{j\ 1,\ldots,n}$ are the weights and $(\mathbf{u}_j)_{j\ 1,\ldots,n}$ are the integration points sometimes called direction cosines (Bažant and Oh, 1986), already defined). The sum of weights must be equal

Table 1
Integral expressions of strain invariants.

Invariant	I_1	I_2	I_3
In terms of λ	$3\langle\lambda^2\rangle$	$3J^3\langle\lambda^5\rangle$	$\langle\lambda^3\rangle^2$
In terms of λ	$3J^1\langle\lambda^5\rangle$	$3J^2\langle\lambda^2\rangle$	$\langle\lambda^3\rangle^2$

to 1 to ensure the exact integration of constant functions, and all weights must be positive in order to provide an upper bound for the error (Hesse et al., 2010).

Here, three particular methods of integration over the microsphere, i.e. methods to derive both $(w_j)_{j\ 1,\dots,n}$ and $(\mathbf{u}_j)_{j\ 1,\dots,n}$, are presented. Obviously, it is not exhaustive but each method can be considered as representative of a given type of approach.

3.1. Method of Bažant and Oh

Bažant and Oh (1986) method is the most classical one for mechanicians: its 42 points (21 points on the hemi sphere) version is the most widely used integration method for constitutive equations; for concrete in micro plane models, and for polymers in microsphere models.

It is a Gaussian integration method, i.e. a method that permits to exactly integrate polynomials of a given degree. Moreover, the authors considered two additional requirements funded on mechanical considerations: first, symmetric formulations are preferred because they respect the symmetry of stress and strain tensors; second, formu lations that minimize the influence of rigid body rotations on the values of integrals are considered. For several num bers of integration points,[2] i.e. 2×21, 2×33, 2×74, 42, 122, the corresponding weights and cosines are given.

3.2. Method of Badel and Leblond

Badel and Leblond (2004) method is a simple meshing approach proposed to overcome the limitations of the pre vious method for some discrepancies in integration of non smooth functions with microplane models.

In a recent paper devoted to constitutive equations for concrete, Badel and Leblond (2004) proposed a different approach for integration over the unit sphere. Following Qiu and Crouch (1997), they noted that the original pro posal of Bažant and Oh (1986) reveals inefficient for some loading conditions and that the generation of higher order Gaussian integration scheme is a "cumbersome task". So the authors propose to develop an automatic strategy that consists in meshing the surface of the unit sphere. Note that this method has been recently used by Levasseur et al. (2013) who demonstrate its relevance for complex structural computations.

As the presentation of the method by authors is clear and concise, we quote it exhaustively (note that it was pro posed for the hemisphere):

> [We] start from the semi dodecahedron with six pen tagonal faces. Each pentagon can be divided into five equal isosceles triangles, their common vertex (centre of the pentagon) being projected radially onto the hemisphere. Each triangle can next be divided into four equal triangles, the newly created vertices (middle points of the original sides) being again pro jected radially onto the hemisphere. (Badel and Leblond, 2004).

Then, the integral of a given function over the unit sphere is obtained by summing, over the triangles, the product area and function value at centroid. Such a method can be easily automated.

The initial mesh consists of 60 triangles (12 pen tagons $\times$ 5 isosceles), and each step multiplies the number of triangles by 4. Thus, the possible numbers of integration points are: 60, 240, 960, 3840, 15,360, 61,440, 245,760, 983,040,..., all weights being equal to the area of triangles.

3.3. Method of Sloan and Womersley

Finally, the Sloan and Womersley (2004) method is rep resentative of modern approaches of cubature used for example in geosciences (Hesse et al., 2010).

The theory is based on spherical harmonics, i.e. the restriction of harmonic and homogeneous polynomials on the unit sphere. Considering the set of all polynomial har monics, denoted $(Y_{l,k})_{l\ 0,1,\dots;k\ 1,\dots,2l+1}$, every square inte grable function on the sphere f can be written as a Fourier series:

$$f \quad \sum_{l\ 0}^{\infty}\sum_{k\ 1}^{2l+1}\alpha_{lk}Y_{l,k}, \tag{37}$$

where $(\alpha_{kl})_{l\ 0,1,\dots;k\ 1,\dots,2l+1}$ are the Fourier coefficients. The spherical harmonics can be expressed in terms of the Legendre polynomials and the trigonometric operators (Sansone, 1959).

Consider now a set of N points $(\mathbf{u}_j)_{j\ 1,\dots,N}$ on the unit sphere and the polynomials of degree $L \geqslant 0$. Then the spherical harmonic basis matrix $\mathbf{Y}$ is defined as the $(L+1)^2\times N$ matrix which elements are $Y_{l,k}(\mathbf{u}_j)$ for $l \quad 0,\dots L$ and $k \quad 1,\dots,2l+1$. Then the method of Sloan and Womersley consists in researching the $(L+1)^2$ points $(\mathbf{x}_j)_{j\ 1,\dots,(L+1)^2}$ that maximizes the determinant of $\mathbf{Y}$ (practi cally, authors consider the symmetric semi definite matrix $\mathbf{G}\quad\mathbf{Y}^T\mathbf{Y}$ rather than $\mathbf{Y}$). The mathematical method employed is not recalled here, but details are given in Sloan and Womersley (2004) and a concise abstract is pro posed by Hesse et al. (2010). As a result, the authors obtained explicit sets of points $(\mathbf{u}_j)$ and their correspond ing weights (w_j) for polynomial degrees up to 165. The data are available in Womersley (2007).

4. Results and discussion

In this section, we first propose a thorough study of the error induced by the choice of the integration method. In this way, the computation of strain invariants

[2] Denoting $2\times\cdot$ signifies that the formulation is fully symmetric and that only the integration over the hemisphere is required.

corresponding to simple deformations is analysed; then depending on the formulation of invariants the appropriate method and the corresponding number of points are deter mined. Second, we apply these results to the classical Mooney Rivlin constitutive equation (written in a direc tional form) to highlight the influence of the integration method on stress strain prediction.

4.1. Errors in strain invariants

We consider two simple deformations:

(i) incompressible 400% uniaxial extension, for which the deformation gradient is

$$\mathbf{F}^{u} \quad 4\,\mathbf{e}_1 \otimes \mathbf{e}_1 + 0.5\,\mathbf{e}_2 \otimes \mathbf{e}_2 + 0.5\,\mathbf{e}_3 \otimes \mathbf{e}_3, \tag{38}$$

where $\mathbf{e}_1$ is the extension direction,

(ii) and incompressible 287.1% equibiaxial extension, the corresponding deformation gradient being

$$\mathbf{F}^{b} \quad 2.871\,\mathbf{e}_1 \otimes \mathbf{e}_1 + 2.871\,\mathbf{e}_2 \otimes \mathbf{e}_2 + 0.1213\,\mathbf{e}_3 \otimes \mathbf{e}_3, \tag{39}$$

where $\mathbf{e}_1$ and $\mathbf{e}_2$ are the in plane extension directions.

In fact, the stretch ratio for the equibiaxial extension has been chosen to produce a deformation with the same value of I_1 than the uniaxial extension deformation. The corresponding values of the strain invariants are

$$I_1^{u} \quad 16.5, \quad I_2^{u} \quad 8.0625, \quad I_3^{u} \quad 1 \tag{40}$$

for uniaxial extension, and

$$I_1^{b} \quad 16.5, \quad I_2^{b} \quad 68.1838, \quad I_3^{b} \quad 1 \tag{41}$$

for equibiaxial extension.

4.1.1. Comparison of the methods

In the following the three integration methods are com pared by calculating the three invariants thanks to formu lae given in Table 1. It is to note here that for the terms that involve J, i.e. I_1 in terms of $\bar{\lambda}$ and I_2 in terms of both λ and $\bar{\lambda}$, it is assumed that $J \quad 1$, such that errors are not accumu lated with potential errors on I_3. Numbers of points adopted for the three methods are given in Table 2.

For each method, the relative errors in the three strain invariants are calculated. The results for the two deforma tions are presented in the same graphs. Considering the highly different numbers of integration points between the methods, results for the Bažant and Oh method are pre sented in linear plots whereas results for the Badel and Leblond, and Sloan and Womersley methods are presented in log log plots. Figs. 3 and 4 present the results for the Bažant and Oh method. As shown in Fig. 3, only I_1 is well predicted by using λ (Eq. (31)); the two others invari ants cannot be calculated whatever the number of integra tion points. Similarly, using $\bar{\lambda}$ (considering $J \quad 1$) permits to precisely evaluate I_2 (Eq. $(35)_2$), but not I_1 and I_3. Moreover, in both cases 42 points, i.e. 21 points on the hemisphere, are sufficient to obtain a relevant estimate. It is in good agreement with the conclusion drawn by Bažant and Oh (1986), and with the choice of the majority of authors who develop microsphere models. Finally, it is to note that the third invariant I_3 cannot be satisfactorily predicted.

Table 2
Number of integration points.

Method	Number of points	Remark
Bažant and Oh	42, 66, 74, 122	divided by 2 because of the symmetry
Badel and Leblond	60, 240, 960, 3840, 15,360, 61,440, 245,760, 983,040	
Sloan and Womersley	from 4 to 27556	$(n+1)^2$ for n from 1 to 165

Figs. 5 and 6 present the results for the Badel and Leblond method. For both deformations, and for all invari ants, choosing λ or $\bar{\lambda}$ leads to similar results: in order to achieve an error of about 0.01%, 245,760 integration points are necessary. Moreover, for more than 240 points, all curves monotonously decrease; it ensures that the increase in discretization of the sphere improves the precision of results.

Finally, Figs. 7 and 8 shows the results for the Sloan and Womersley method. Similar trends than with the Bažant and Oh method are obtained: formulae in terms of λ, respectively in terms of $\bar{\lambda}$, permit to precisely calculate I_1 (see left hand side graph in Fig. 7), respectively I_2 (see mid dle graph in Fig. 8), with a very high precision and only few integration points. Moreover, the four other graphs are similar: the error decreases with the number of points, and whatever the invariant and the deformation about 10^4 integration points lead to errors less than 0.01%.

4.1.2. Choice of the relevant method

In order to give quantitative results, the number of inte gration points that is necessary to ensure convergence of computations for each method is discussed. In this way, the precision is prescribed; then for each integration method, we compute the minimum number of integration points such that convergence on all invariants for both deformations is achieved. First, we consider the cases where the three invariants are computed with λ using Eqs. (31), $(35)_1$ and $(36)_1$, and with $\bar{\lambda}$ using Eqs. (30), $(35)_2$ and $(36)_2$. The corresponding results are presented in Tables 3 and 4, respectively. First, we note that the Bažant and Oh method does not permit to calculate the invariants even for an error of 10%. Second, it appears that the computation of invariants necessitates less integration points in terms of $\bar{\lambda}$ than in terms of λ for both Badel and Leblond, and Sloan and Womersley methods. Third, the Sloan and Womersley method is revealed highly more effi cient than the Badel and Leblond method: depending on the error value, it necessitates between 4 and 90 times less integration points. Note that for 0.01% error and computa tion with λ, only the Badel and Leblond method converges with 983,040 integration points. To retain only one result, we show that more than 6000 integration points (with the Sloan and Womersley method) are necessary to achieve a

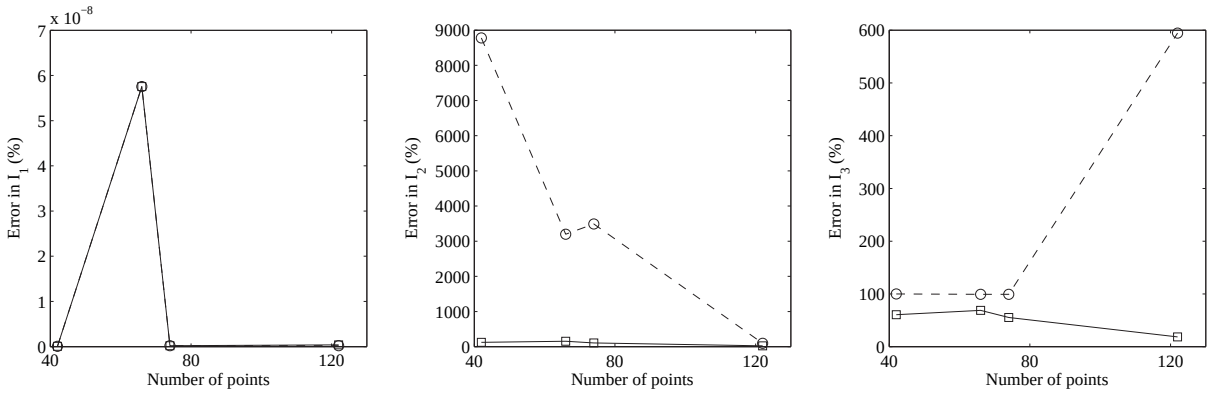

Fig. 3. Error in strain invariants calculated in terms of λ with the method of Bažant and Oh. □: uniaxial tension, ◯: equibiaxial extension.

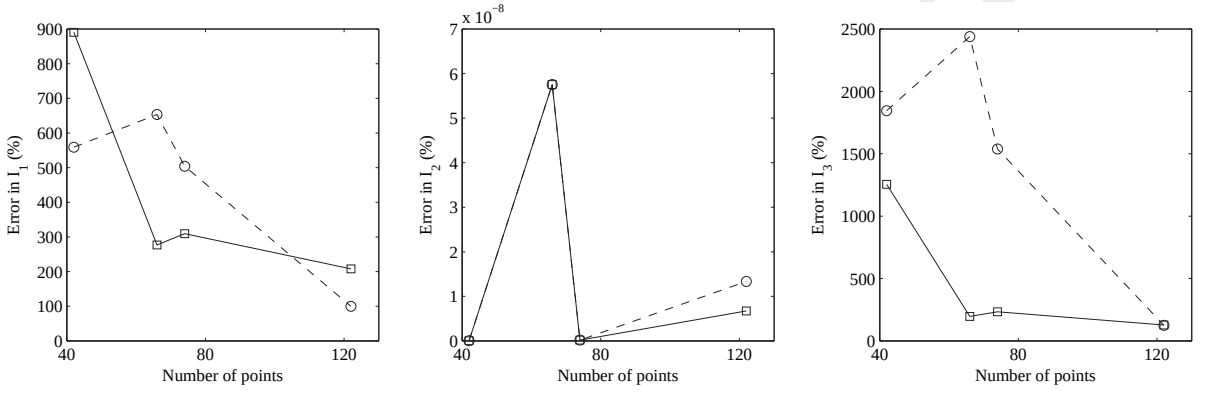

Fig. 4. Error in strain invariants calculated in terms of λ with the method of Bažant and Oh. □: uniaxial tension, ◯: equibiaxial extension.

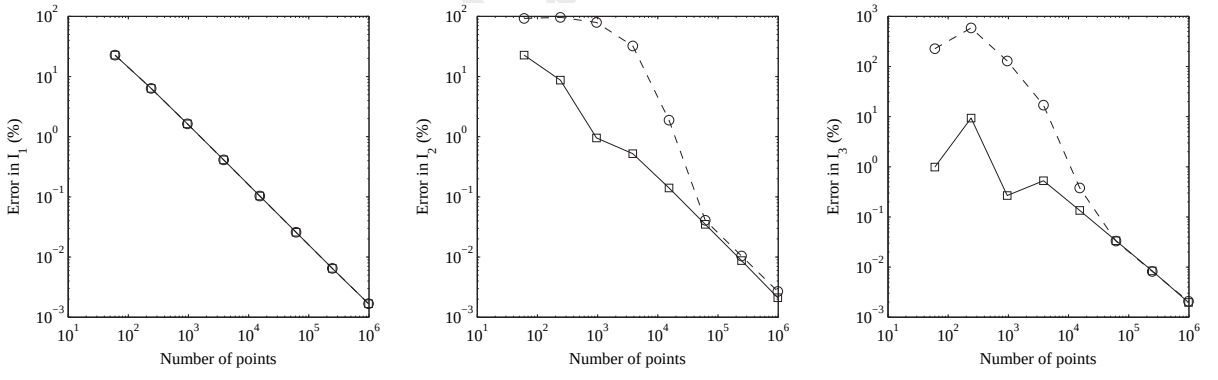

Fig. 5. Error in strain invariants calculated in terms of λ with the method of Badel and Leblond. □: uniaxial tension, ◯: equibiaxial extension.

1% convergence on all invariants computed in terms of λ (see Table 3). This result questions the validity of predic tions of numerous recently developed microsphere consti tutive equations in which complex functions of λ are involved.

We consider now the cases in which both λ and $\bar{\lambda}$ are used to evaluate the invariants. Two cases are investigated: compressible materials for which I_3 must be evaluated (see Table 5) and incompressible materials for which only I_1 an I_2 must be calculated (see Table 6). In the former case, the Bažant and Oh method is not able to calculate the invari ants; for both Badel and Leblond, and Sloan and Womersley methods, the necessary number of integration points is reduced as compared to the computations with λ or $\bar{\lambda}$ only. The latter case is representative of the majority of microsphere models which are incompressible, and for which the incompressibility constraint is treated macro scopically by separating the stress into a deviatoric part

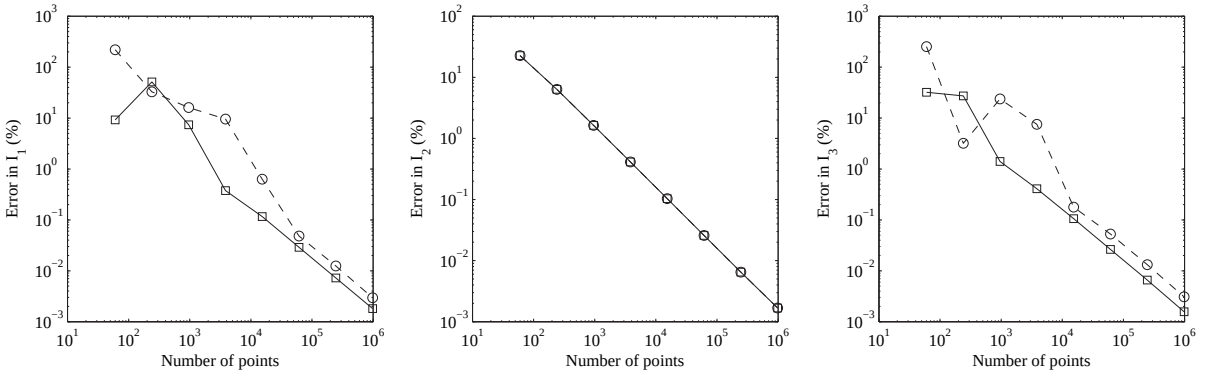

Fig. 6. Error in strain invariants calculated in terms of λ with the method of Badel and Leblond. □: uniaxial tension, ○: equibiaxial extension.

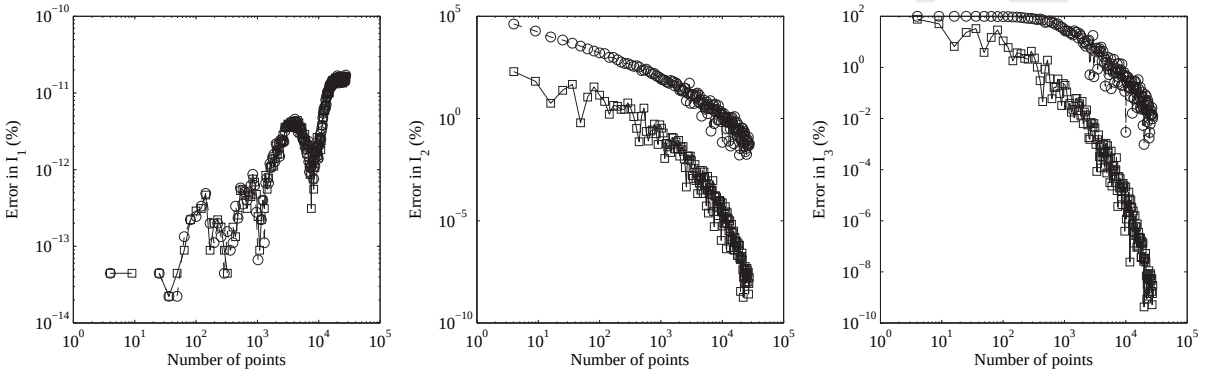

Fig. 7. Error in strain invariants calculated in terms of λ with the method of Sloan and Womersley. □: uniaxial tension, ○: equibiaxial extension.

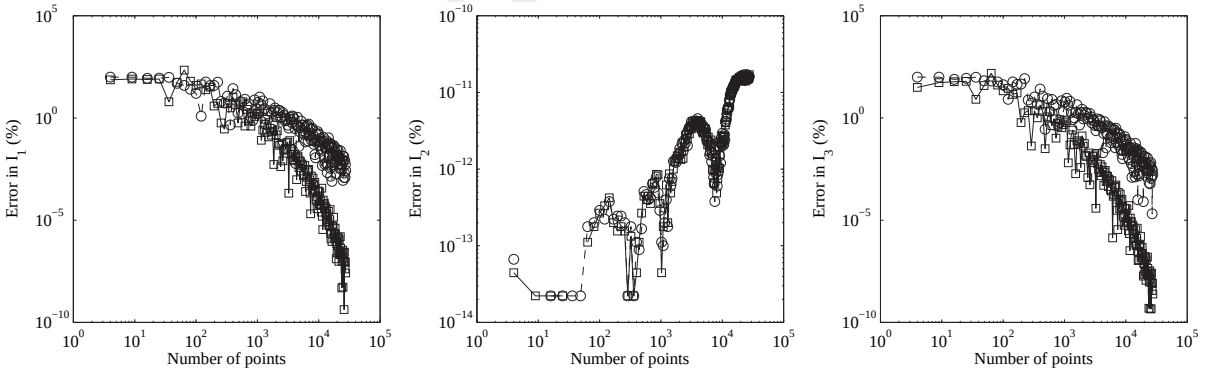

Fig. 8. Error in strain invariants calculated in terms of λ with the method of Sloan and Womersley. □: uniaxial tension, ○: equibiaxial extension.

Table 3
Number of integration points necessary to ensure convergence of all invariants computed with λ.

Precision (%)	Bažant and Oh	Badel and Leblond	Sloan and Womersley
10	×	15,360	2601
5	×	15,360	4624
1	×	61,440	6561
0.1	×	61,440	10,000
0.01	×	983,040	×

Table 4
Number of integration points necessary to ensure convergence of all invariants computed with λ.

Precision (%)	Bažant and Oh	Badel and Leblond	Sloan and Womersley
10	×	3840	121
5	×	15,360	361
1	×	15,360	484
0.1	×	61,440	4225
0.01	×	983,040	11,449

Table 5
Number of integration points necessary to ensure convergence of all invariants computed with both λ and λ; i.e. compressible case $I_3 \neq 1$

Precision (%)	Bažant and Oh	Badel and Leblond	Sloan and Womersley
10	×	960	121
5	×	960	361
1	×	15,360	2601
0.1	×	61,440	4225
0.01	×	245,760	10,000

computed by integration over the sphere and a spherical part encompassed in an arbitrary pressure. In this case, the Bažant and Oh method with 42 points (21 on the hemi sphere) is relevant. The Badel and Leblond method neces sitates almost the same number of points than in the compressible case especially for small errors. Finally, the Sloan and Womersley method reveals highly surprising results and proves its efficiency: only 4 integration points are necessary to achieve convergence with 0.01% error!

4.2. Application to stress strain prediction

In order to illustrate the possible consequences of an inappropriate choice of the integration method on stress strain prediction, we consider the most classical hyperelas tic model for rubber like materials: the incompressible Mooney Rivlin model (Mooney, 1940; Rivlin, 1948; Treloar, 1975; Marckmann and Verron, 2006). It is defined by two material parameters C_1 and C_2 such that the strain energy density is

$$W(\mathbf{C}) \quad C_1(I_1 \quad 3) + C_2(I_2 \quad 3). \tag{42}$$

As the incompressibility assumption is adopted, only deformations such that $I_3 \quad \det \mathbf{C} \quad 1$ are considered. In order to simplify the discussion, we consider the reduced strain energy function $\widetilde{W} \quad W/2C_1$ defined as

$$\tilde{W}(\mathbf{C}) \quad \frac{1}{2}[(I_1 \quad 3) + \alpha(I_2 \quad 3)], \tag{43}$$

where $\alpha \quad C_2/C_1$ is the unique material parameter. Introducing the arbitrary pressure p due to the incom pressibility constraint, the first Piola Kirchhoff (nominal) stress tensor is given by

$$\mathbf{P} \qquad p\mathbf{F}^{\ T} + \frac{\partial \widetilde{W}}{\partial \mathbf{F}} \qquad p\mathbf{F}^{\ T} + (1 + \alpha I_1)\mathbf{F} \quad \alpha \mathbf{F}\mathbf{C}. \tag{44}$$

Several directional versions of the Mooney Rivlin model have been recently proposed (Carol et al., 2004; Lion et al., 2013). Here, we simply incorporate definitions of I_1 and I_2 in terms of the directional stretch $\lambda(\mathbf{u})$, i.e. Eqs. $(31)_3$ and $(35)_1$ with $J \quad 1$ respectively, into the defini tion of $\widetilde{W}$:

$$\widetilde{W}(\mathbf{C}) \quad \frac{1}{2}\left[3\left(\langle \lambda^2 \rangle \quad 1\right) + 3\alpha\left(\langle \lambda^{\ 5} \rangle \quad 1\right)\right] \quad \left\langle \frac{3}{2}\left(\lambda^2 + \alpha\lambda^{\ 5}\right) \right\rangle \quad \frac{3}{2}(1+\alpha). \tag{45}$$

Introducing the standard notations, one can identify a sort of *Mooney chain energy* for the chain oriented in direction $\mathbf{u}$

$$w(\lambda(\mathbf{u})) \quad \frac{3}{2}\left(\lambda(\mathbf{u})^2 + \alpha\lambda(\mathbf{u})^{\ 5}\right) \tag{46}$$

and the constant $3(1+\alpha)/2$ which nullifies the strain energy in the undeformed state. Thus, the corresponding derivation of the first Piola Kirchhoff stress tensor in Eq. $(44)_1$ necessitates the following quantity

$$\frac{\partial \widetilde{W}}{\partial \mathbf{F}} \quad \left\langle \frac{\partial w(\lambda(\mathbf{u}))}{\partial \mathbf{F}} \right\rangle \quad \left\langle \frac{dw(\lambda(\mathbf{u}))}{d\lambda} \frac{\partial \lambda(\mathbf{u})}{\partial \mathbf{F}} \right\rangle \quad \left\langle \left(3\lambda(\mathbf{u}) \quad \frac{15}{2}\alpha\lambda(\mathbf{u})^{\ 6}\right) \frac{1}{\lambda(\mathbf{u})} \mathbf{F}\mathbf{u} \otimes \mathbf{u} \right\rangle \quad \mathbf{F}\left\langle \left(3 \quad \frac{15}{2}\alpha\lambda(\mathbf{u})^{\ 7}\right) \mathbf{u} \otimes \mathbf{u} \right\rangle. \tag{47}$$

And finally,

$$\mathbf{P} \qquad p\mathbf{F}^{\ T} + \mathbf{F} \quad \frac{15}{2}\alpha\mathbf{F}\left\langle \lambda(\mathbf{u})^{\ 7}\mathbf{u} \otimes \mathbf{u} \right\rangle. \tag{48}$$

For the numerical examples, we set $\alpha \quad 0.25$ and con sider two deformations: uniaxial extension such that

$$\mathbf{F} \quad \Lambda\, \mathbf{e}_1 \otimes \mathbf{e}_1 + \Lambda^{\ 1/2}\mathbf{e}_2 \otimes \mathbf{e}_2 + \Lambda^{\ 1/2}\mathbf{e}_3 \otimes \mathbf{e}_3 \tag{49}$$

and equibiaxial extension such that

$$\mathbf{F} \quad \Lambda\, \mathbf{e}_1 \otimes \mathbf{e}_1 + \Lambda\, \mathbf{e}_2 \otimes \mathbf{e}_2 + \Lambda^{\ 2}\mathbf{e}_3 \otimes \mathbf{e}_3. \tag{50}$$

Applying Eq. (44) and eliminating the pressure p with $P_{33} \quad 0$ respectively leads to the uniaxial stress strain relationship

$$P \quad \left(\Lambda \quad \frac{1}{\Lambda^2}\right)\left(1 + \alpha\frac{1}{\Lambda}\right), \tag{51}$$

the tensor $\mathbf{P}$ being $\mathbf{P} \quad P\,\mathbf{e}_1 \otimes \mathbf{e}_1$, and the equibiaxial stress strain relationship

$$P \quad \left(\Lambda \quad \frac{1}{\Lambda^5}\right)\left(1 + \alpha\Lambda^2\right), \tag{52}$$

the tensor $\mathbf{P}$ being $\mathbf{P} \quad P(\mathbf{e}_1 \otimes \mathbf{e}_1 + \mathbf{e}_2 \otimes \mathbf{e}_2)$. The directional counterparts of these equations are computed by consider ing the corresponding deformation gradient (Eq. (49) or (50)), the stress strain relationship Eq. (48) and the plane stress condition $P_{33} \quad 0$ that permits to calculate the pres sure p.

For uniaxial tension the results are presented in Fig. 9 for the three methods and some representative numbers of integration points. The results for equibiaxial tension are shown in Fig. 10. Results confirm our previous

Table 6
Number of integration points necessary to ensure convergence of I_1 and I_2 computed with both λ and λ; i.e. incompressible case $I_3 \quad 1$.

Precision (%)	Bažant and Oh	Badel and Leblond	Sloan and Womersley
10	42	240	4
5	42	960	4
1	42	3840	4
0.1	42	61,440	4
0.01	42	245,760	4

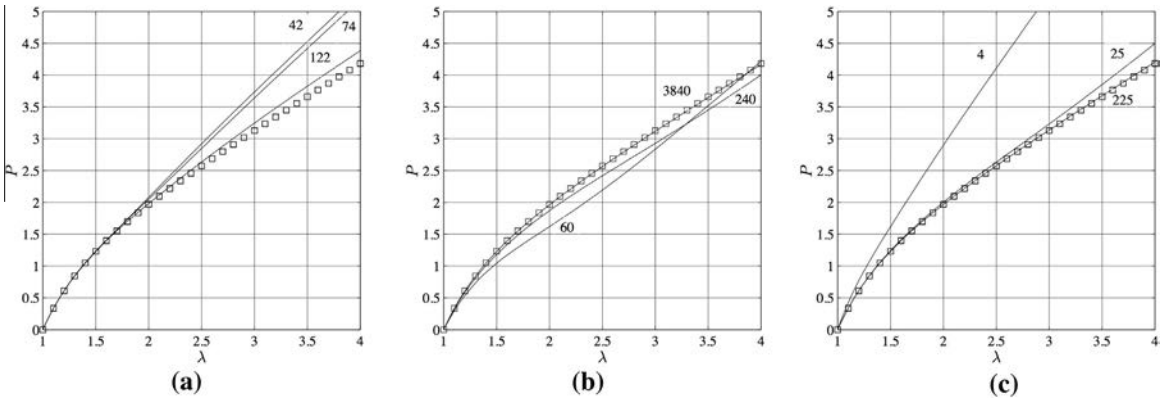

Fig. 9. Response of the Mooney–Rivlin model ($\alpha \quad C_2/C_1 \quad 0.25$) in uniaxial tension; number of points are given for each curve: (a) Bažant and Oh method, (b) Badel and Leblond method, (c) Sloan and Womersley method.

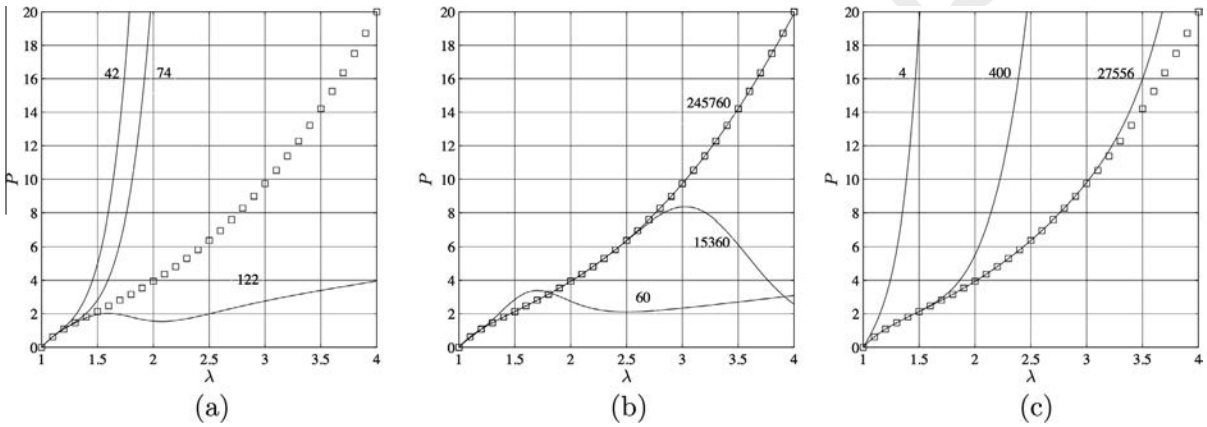

Fig. 10. Response of the Mooney-Rivlin model ($\alpha \quad C_2/C_1 \quad 0.25$) in equibiaxial tension; number of points are given for each curve: (a) Bažant and Oh method, (b) Badel and Leblond method, (c) Sloan and Womersley method.

discussion. Indeed, the Bažant and Oh method is unable to predict the stress strain response. In uniaxial tension, both Badel and Leblond, and Sloan and Womersley methods are successful, respectively with 3840 and 225 points, as shown in Fig. 9(a) and (b). Predictions in equibiaxial tension are more disturbing. Only the Badel and Leblond method with 245,760 integration points is revealed able to predict the Mooney Rivlin stress strain response (see Fig. 10(b)). Moreover numerical predictions can conduct to major mistakes: the Badel and Leblond method leads to non monotonic curves (60 and 15,360 points in Fig. 10(b)), the Sloan and Womersley method leads to wrong strain stiffening responses (for the three number of points tested, see Fig. 10 (c)), and the Bažant and Oh method can lead to these two types of error depending on the number of points as shown in Fig. 10(a). In fact, these results confirm that the cubature method and the number of integration points must be carefully chosen even for simple constitutive equations written in a directional form.

5. Closure

In this paper, integration methods over the unit sphere have been investigated through the computation of principal strain invariants for simple deformations. Even if the results are partial (only three methods and two deformations), some conclusions can be drawn. Indeed, the principal invariants are intrinsically involved in consti tutive equations: I_1 in all models and I_2 in tube like approaches (Ehret, 2015). First, the standard Bažant and Oh method is revealed insufficient in most of the cases. Second, the Badel and Leblond method has led to conver gence whatever the precision for cases studied here, but it necessitates a large number of integration points. Third, the Sloan and Womersley method has proved its efficiency in all cases except one, with sometimes a very few number of integration points. Application to the simple hyperelastic Mooney Rivlin model has confirmed the results highlighted with invariants. Moreover it has demonstrated that a bad choice of the integration method

leads to large errors in stress strain prediction. All these results can be partially explained by the inability of stan dard methods to handle non smooth functions even with a large number of integration points as previously empha sized by Badel and Leblond (2004).

Finally, some remarks can be proposed for the develop ment of new microsphere constitutive equations.

- The choice of the integration method and the determi nation of the relevant number of points must be consid ered as a part of the derivation of the constitutive equation.
- For a given constitutive equation, the Badel and Leblond method with a very large number of integration points can be used to obtain the reference solution. Once this solution calculated, the Sloan and Womersley method can be investigated to determine the relevant number of integration points (if possible). For the purpose, sev eral simple and complex deformations must be considered.
- Formulations in terms of both λ, i.e. $\|\mathbf{Fu}\|$, and $\bar{\lambda}$, i.e. $\|\mathbf{F}^{T}\mathbf{u}\|$, have to be considered in order to reduce the number of integration points. In this way, the smooth ness of functions to be integrated must be carefully studied.
- For incompressible models involving only I_1, it is possi ble to consider only few integration points, for example with the 21 points of the Bažant and Oh method. Nevertheless, the development of compressible micro sphere equations necessitates a high number of integra tion points, e.g. 2601 points with the Sloan and Womersley method for a 1% error; then it will necessi tate particular studies devoted to computing time.

References

Alastrué, V., Martinez, M., Doblaré, M., Menzel, A., 2009. Anisotropic micro-sphere-based finite elasticity applied to blood vessel modelling. J. Mech. Phys. Solids 57, 178–203.

Alastrué, V., Martinez, M.A., Menzel, A., Doblaré, M., 2009. On the use of non-linear transformations for the evaluation of anisotropic rotationally symmetric directional integrals. Application to the stress analysis in fibred soft tissues. Int. J. Numer. Methods Eng. 79, 474–504.

Arruda, E.M., Boyce, M.C., 1993. A three dimensional constitutive model for the large stretch behavior of rubber elastic materials. J. Mech. Phys. Solids 41 (2), 389–412.

Badel, P.-B., Leblond, J.-B., 2004. A note on integration schemes for the microplane model of the mechanical behaviour of concrete. Commun. Numer. Methods Eng. 20, 75–81.

Bažant, Z.P., Caner, F.C., Carol, I., Adley, M.D., Akers, S.A., 2000. Microplane model M4 for concrete. I: Formulation with work-conjugate deviatoric stress. J. Eng. Mech.-ASCE 126 (9), 944–953.

Bažant, Z.P., Gambarova, P.G., 1984. Crack shear in concrete – crack band microplane model. J. Struct. Eng.-ASCE 110 (9), 2015–2035.

Bažant, Z.P., Oh, B.H., 1985. Microplane model for progressive fracture of concrete and rock. J. Eng. Mech.-ASCE 111 (4), 559–582.

Bažant, Z.P., Oh, B.H., 1986. Efficient numerical integration on the surface of a sphere. Z. Angew. Math. Mech. 66, 37–49.

Bažant, Z.P., Prat, P.C., 1988. Microplane model for brittle-plastic material. 1. Theory. J. Eng. Mech.-ASCE 114 (10), 1672–1687.

Beatty, M.F., 2003. An average-stretch full-network model for rubber elasticity. J. Elast. 70, 65–86.

Brocca, M., Bažant, Z.P., 2000. Microplane constitutive model and plasticity. Appl. Mech. Rev. 50 (10), 265–281.

Carol, I., Bažant, Z.P., 1997. Damage and plasticity in microplane theory. Int. J. Solids Struct. 34 (29), 3807–3835.

Carol, I., Jirásek, M., Bažant, Z.P., 2004. A framework for microplane models at large strain, with application to hyperelasticity. Int. J. Solids Struct. 41, 511–557.

Cheng, W., Shen, Z., 2010. An improved method to calculate the directions and weights in microplane constitutive model. In: Oh, B.H. et al. (Ed.), Recent Advances in Fracture Mechanics of Concrete, pp. 635–643.

Dal, H., Kaliske, M., 2009. A micro-continuum-mechanical material model for failure of rubber-like materials: application to ageing-induced fracturing. J. Mech. Phys. Solids 57 (8), 1340–1356.

Dargazany, R., Itskov, M., 2009. A network evolution model for the anisotropic Mullins effect in carbon black filled rubbers. Int. J. Solids Struct. 46, 2967–2977.

Diani, J., Brieu, M., Vacherand, J.-M., 2006. A damage directional constitutive model for Mullins effect with permanent set and induced anisotropy. Eur. J. Mech. A/Solids 25, 483–496.

Ehret, A.E., 2015. On a molecular statistical basis for Ogden's model of rubber elasticity. J. Mech. Phys. Solids. http://dx.doi.org/10.1016/j.jmps.2015.02.006.

Ehret, A.E., Itskov, M., Schmid, H., 2010. Numerical integration on the sphere and its effect on the material symmetry of constitutive equations – a comparative study. Int. J. Numer. Methods Eng. 81, 189–206.

Fleischhauer, R., Dal, H., Kaliske, M., Schneider, K., 2012. A constitutive model for finite deformation of amorphous polymers. Int. J. Mech. Sci. 65 (1), 48–63.

Flory, P.J., Rehner, J., 1943. Statistical mechanics of cross-linked polymer networks. I. Rubberlike elasticity. J. Chem. Phys. 11, 512–520.

Gillibert, J., Brieu, M., Diani, J., 2010. Anisotropy of direction-based constitutive models for rubber-like materials. Int. J. Solids Struct. 47, 640–646.

Gurtin, M.E., Fried, E., Anand, L., 2010. The Mechanics and Thermodynamics of Continua. Cambridge University Press.

Hesse, K., Sloan, I.H., Womersley, R.S., 2010. Numerical integration on the sphere. In: Freeden, W., Nashed, M.Z., Sonar, T. (Eds.), Handbook of Geomathematics. Springer, pp. 1187–1219, Ch. 40.

James, H.M., Guth, E., 1943. Theory of the elastic properties of rubber. J. Chem. Phys. 11, 455–481.

Kearsley, E.A., 1989. Note: strain invariants expressed as average stretches. J. Rheol. 33 (5), 757–760.

Levasseur, S., Collin, F., Charlier, R., Kondo, D., 2013. On micromechanical damage modeling in geomechanics: influence of the numerical integration scheme. J. Comput. Appl. Math. 246, 215–224.

Lion, A., Diercks, N., Caillard, J., 2013. On the directional approach in constitutive modelling: a general thermomechanical framework and exact solutions for Mooney–Rivlin type elasticity in each direction. Int. J. Solids Struct. 50, 2518–2526.

Marckmann, G., Verron, E., 2006. Comparison of hyperelastic models for rubberlike materials. Rubber Chem. Technol. 79, 835–858.

Miehe, C., Göktepe, S., Lulei, F., 2004. A micro-macro approach to rubber-like materials – Part I: The non-affine micro-sphere model of rubber elasticity. J. Mech. Phys. Solids 52, 2617–2660.

Mistry, S.J., Govindjee, S., 2014. A micro-mechanically based continuum model for strain-induced crystallization in natural rubber. Int. J. Solids Struct. 51 (2), 530–539.

Mooney, M., 1940. A theory of large elastic deformation. J. Appl. Phys. 11, 582–592.

Puso, M., 2003. Mechanistic Constitutive Models for Rubber Elasticity and Viscoelasticity (Ph.D. thesis). University of California, Davis, USA.

Qiu, Y., Crouch, R.S., 1997. Spurious compaction in the microplane model and new adaptative framework. In: Owen, D.R.J., Oñate, E., Hinton, E. (Eds.), Computational Plasticity. CIMNE, Barcelona, pp. 493–499.

Rebouah, M., Chagnon, G., 2014. Extension of classical viscoelastic models in large deformation to anisotropy and stress softening. Int. J. Non-Linear Mech. 61, 54–64.

Rebouah, M., Chagnon, G., 2014. Permanent set and stress-softening constitutive equation applied to rubber-like materials and soft tissues. Acta Mech. 225 (6), 1685–1698.

Rivlin, R.S., 1948. Large elastic deformation of isotropic materials – IV. Further developments of the general theory. Philos. Trans. R. Soc. A 241, 379–397.

Sansone, G., 1959. Orthogonal Functions. Interscience Publishers, London, New-York.

Sloan, I.H., Womersley, R.S., 2004. Extremal systems of points and numerical integration on the sphere. Adv. Comput. Math. 21, 107–125.

Tkachuk, M., Linder, C., 2012. The maximal advance path constraint for the homogenization of materials with random network microstructure. Philos. Mag. 92 (22), 2779–2808.

Treloar, L.R.G., 1975. The Physics of Rubber Elasticity. Oxford University Press, Oxford.
Treloar, L.R.G., Riding, G., 1979. A non-Gaussian theory for rubber in biaxial strain. I. Mechanical properties. Proc. R. Soc. Lond. A 369, 261–280.
Womersley, R.S., 2007. Interpolation and cubature on the sphere. URL <http://web.maths.unsw.edu.au/rsw/Sphere/>.
Wu, P.D., van der Giessen, E., 1993. On improved network models for rubber elasticity and their applications to orientation hardening in glassy polymers. J. Mech. Phys. Solids 41 (3), 427–456.
Zäh, D., Miehe, C., 2015. Multiplicative electro-elasticity of electroactive polymers accounting for micromechanically-based network models. Comput. Methods Appl. Mech. Eng. 286, 394–421.